Effect of zinc coating on the fretting fatigue endurance of crossed steel wires

Sébastien Montalvo, Siegfried Fouvry, Michaël Martinez

Effect of zinc coating on the fretting fatigue endurance of crossed steel wires

Sébastien Montalvo [a,b], Siegfried Fouvry [a], Michaël Martinez [b]

[a] Laboratoire de Tribologie et de Dynamique des Systèmes, Centrale Lyon, 36 Av. Guy de Collongue, 69134 Écully, France

[b] IFP Energies Nouvelles, Rond point de l'échangeur de Solaize, 69360 Solaize, France

Corresponding authors: Siegfried Fouvry (siegfried.fouvry@ec-lyon.fr); Sébastien Montalvo, (sebastien.montalvo@gmail.com); Michaël Martinez (michael.martinez@ifpen.fr).

Keywords:

Fretting fatigue, steel wires, zinc coating, galvanisation

Abstract:

Fretting fatigue causes failures in steel wire ropes. These steel wires are usually galvanised. This zinc coating could change the crack initiation process, as it modifies the contact interface. In this study, fretting fatigue tests were performed on bright (non galvanised) and galvanised wires under ambiant air, varying independantly fretting and fatigue loadings. No significative beneficial effect of galvanisation on lifetimes was observed, contrary to what was found in litterature. Plain fretting tests and dedicated observations were performed to better interpret the influence of zinc coating.

1. Introduction

Steel wire ropes can be used as floating offshore wind turbines mooring lines. They are composed of steel wires helically wound around a central wire, organised in successive layers. The directions of the helix alternates between each layer, producing punctual contacts between the wires ("treillis" contact). The sea swell induces tensile and bending cyclic loads on the rope. The cyclic tension generates cyclic stress in the bulk of the wires, which can cause *fatigue*, i.e. the initiation and

propagation of cracks in the wires until failure. The cyclic bending induces small relative displacements between the wires in contact, i.e. *fretting*. This generates high local stresses at the contact location, promoting faster crack initiation. Fretting induced cracks can then propagate because of the fatigue load. This phenomenon called *fretting fatigue* is more damaging than plain fretting or plain fatigue, and has been widely studied [8, 15, 24, 26]. Raoof and his coworkers have shown that fretting fatigue damage at treillis contacts is the main factor controlling the rope fatigue life [9, 19–21]. The steel wires are usually galvanised (application of a zinc coating) as a protection against corrosion [1]. Dieng *et al.* [4] studied the effects of zinc coating on steel wires fretting fatigue damage. Using a single actuator testing machine (the fretting and fatigue loads were thus coupled), they applied a 200 N constant normal force and fatigue loads with stress range varying from 50 MPa to 300 MPa. They found a significative improvement of the fretting fatigue limit for Zn coated wires compared to bright wires: respectively 170 MPa and 100 MPa at 10^7 cycles. Note that the fretting fatigue limits are expressed in stress ranges, so that they correspond to limits of respectively 85 MPa and 50 MPa when expressed in stress amplitudes. Dieng *et al.* observed an increase in the contact area for coated wires compared to bright wires, and made the hypothesis that this would reduce the contact stresses and thus increase the fretting fatigue limit. They applied a mechanical model which predicted that the softer zinc would plastically flow out of the contact area, thus inducing a larger contact area. Ramalho *et al.* [18] studied the effect of zinc coating on the fretting fatigue behavior of steel sheets and found that it markedly improved the fracture life. While they observed oxydes and adhesion damage on uncoated specimens, they report that the coated specimens are smooth and show no significant surface damage. Regalla *et al.* [22] studied the tribological behavior of zinc coating on steel with a pin-on-disc setup. They found a beneficial effect on wear damage, but also that the coating was rapidly worn out. Lee *et al.* [11] studied the fretting behaviors of Cd and ZnNi coatings. They explain several mechanisms of wear and velocity accomodation in the case of soft coatings, using the third body formalism of Denape *et al.* [2].

This study aims at investigating the effects of zinc coating on steel wires fretting fatigue endurance. In the present investigation, the applied fretting fatigue loads correspond to the loads in an inner layer of a large diameter spiral strand rope used in tension leg platforms composed of over 300 wires arranged in 12 layers. This technology requires very stiff ropes which are normally only loaded in tension. Yet their behaviour is presently investigated in the case of some additional cyclic bending, which leads to relative movement between the wires and thus fretting fatigue. The loads were calculated using an analytical model and a numerical simulation. The loads applied by Dieng *et al.* correspond to the loads in the outer layers of civil engineering ropes (typically hangers of suspension bridges), which have smaller diameters. For this reason, the loads applied here differ from the ones

applied by Dieng *et al.* Plain fretting and fretting fatigue tests were conducted on bright and coated wires, and then observed. Several results on the bright wires were extracted from previous research works we conducted [14], and the numerical method developped in this research works to predict fretting fatigue crack initiation was here applied to coated wires. The wires in steel ropes used offshore are not only zinc coated but also greased. However, to isolate the effect of the zinc layer, the grease is disregarded in the present paper.

2. Material and methods

2.1. Materials

The studied specimens are 4.85 mm in diameter high strength steel wires. The coating is 50 µm thick, and is composed of 5% aluminium and 95% zinc. Figure 1.a displays a transverse section of a coated wire, showing the steel core and the coating. The coating is composed of an outer layer of zinc alloy and an intermediary 10 µm layer of Zn-Fe compound. This compound layer is mentionned in several works investigating the structure of galvanised steel wires [3, 25]. We also prepared bright wires specimens, removing the coating using inhibited hydrochloric acid. Figure 1.b displays a transverse section of a bright wire specimen.

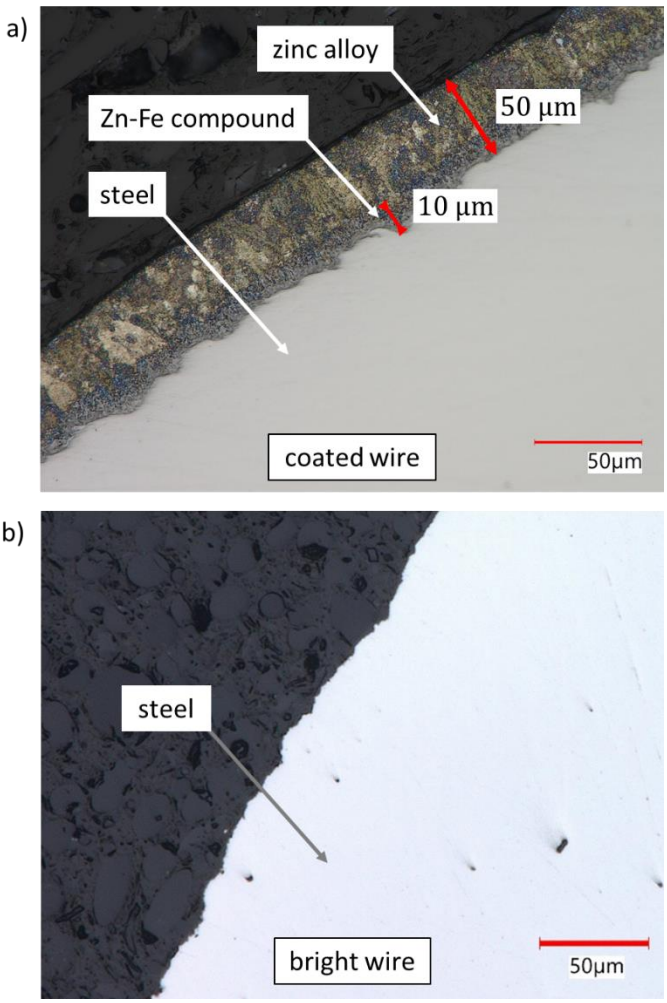

Figure 1 : a) transverse section of a coated wire, b) transverse section of a bright wire, after removal of the coating

The material properties of the steel are listed in Table 1. The exact chemical composition cannot be provided, but the ranges for the main elements prescribed by the standard are reproduced. The elasticity modulus was supplied by the manufacturer, while the yield stress was obtained through several traction tests and the fatigue limit through fatigue tests.

Table 1 : material properties of the steel

Elasticity modulus E	210 GPa

Yield stress	1800 MPa									
Fatigue limit in pure alternated tension σ_D	850 MPa									
Chemical composition ranges (%)	Steel grade C92D (standard ISO 16120-2 [27])									
	C	Si	Mn	P	S	Cr	Ni	Mo	Cu	Al
	0.90 to 0.95	0.10 to 0.30	0.50 to 0.80	0.030 max	0.030 max	0.15 max	0.20 max	0.05 max	0.25 max	0.01 max

2.2. Test rig and protocols

Figure 2 displays the MTS hydraulic rig on which the tests were conducted. It is based on a "double actuator" concept [5, 13], which allows to investigate the influence of a load (fretting or fatigue) while keeping the other constant.

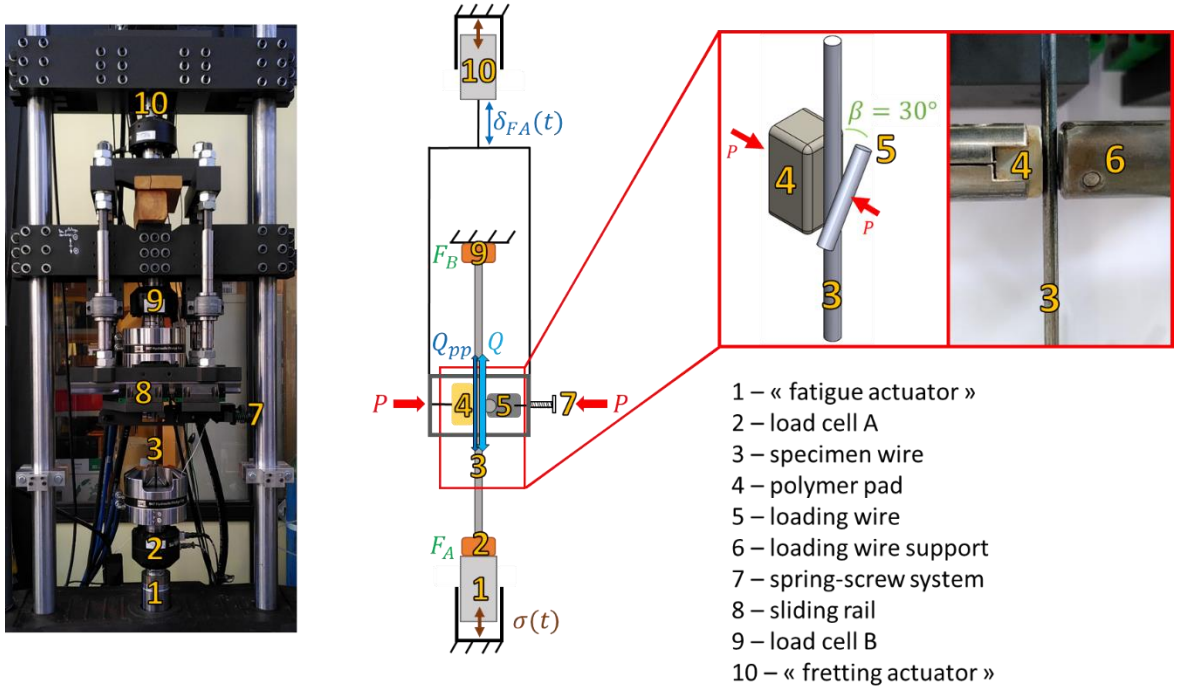

Figure 2 : fretting fatigue test rig

A "fatigue actuator" applies a cyclic force $F_A(t)$ to the specimen wire. Load cells A and B measure the forces F_A and F_B on both extremities of the specimen. The fatigue load is given by:

$$\sigma(t) = \frac{F_B(t)}{S} = \sigma_m + \sigma_a \cdot \sin(2\pi f t) \quad (1)$$

where *S* is the specimen cross-section area and *f* is the actuator's frequency.

A loading wire is put in contact with the specimen wire at a $\beta = 30°$ angle, which corresponds to the angle in the studied wire rope. A constant normal force *P* is applied on the specimen wire through the loading wire. On the opposite side of the specimen wire, a polymer pad prevents the bending of the specimen wire under the normal force. The "fretting actuator" displacement $\delta_{FA}(t) = \delta_{FA}^* \cdot \sin(2\pi f t)$ induces a fretting load $Q(t) = Q^* \cdot \sin(2\pi f t)$ on the specimen wire through the loading wire. The two actuators run at the same frequency and are in phase.

The amplitude of the fretting load Q^* is obtained thanks to the measurements of load cells A and B and a calculation taking into account the friction force between the polymer pad and the specimen wire Q^*_{pp}:

$$Q^* = F_B^* - F_A^* - Q_{pp}^* \quad (2)$$

The friction coefficient of the contact between the polymer pad and the specimen wire μ_{pp} = 0.07 and the displacement amplitude at the partial slip to gross slip transition $\delta^*_{FA,t,pp}$ = 20 µm were obtained thanks to plain fretting tests with two polymer pads on each side of the specimen wire. The friction force amplitude between the polymer pad and the specimen wire Q^*_{pp} is thus equal to:

$$Q_{pp}^*(\delta_{FA}^*) = \begin{cases} \delta_{FA}^* \cdot \dfrac{\mu_{pp} \cdot P}{\delta_{FA,t,pp}^*} & \text{if } \delta_{FA}^* \leq \delta_{FA,t,pp}^* \text{ (partial slip in the polymer pad contact)} \\ \mu_{pp} \cdot P & \text{if } \delta_{FA}^* > \delta_{FA,t,pp}^* \text{ (gross slip in the polymer pad contact)} \end{cases} \quad (3)$$

For a better readibility of the figures, we will use the (effective) displacement amplitude defined by:

$$\delta^* = \delta_{FA}^* - \delta_{FA,0}^* \quad (4)$$

where $\delta^*_{FA,0}$ is the displacement amplitude of the fretting actuator when the elongation of the specimen due to the fatigue amplitude load is fully compensated (so that $Q^* = 0$). Equation (3) can be applied when $\delta^*_{FA,0}$ is not null simply by remplacing δ^*_{FA} by $|\delta^*|$. This calculation is illustrated in Figure 3, which displays the tangential force amplitude in function of the fretting actuator displacement amplitude during a variable displacement amplitude test with a fatigue load.

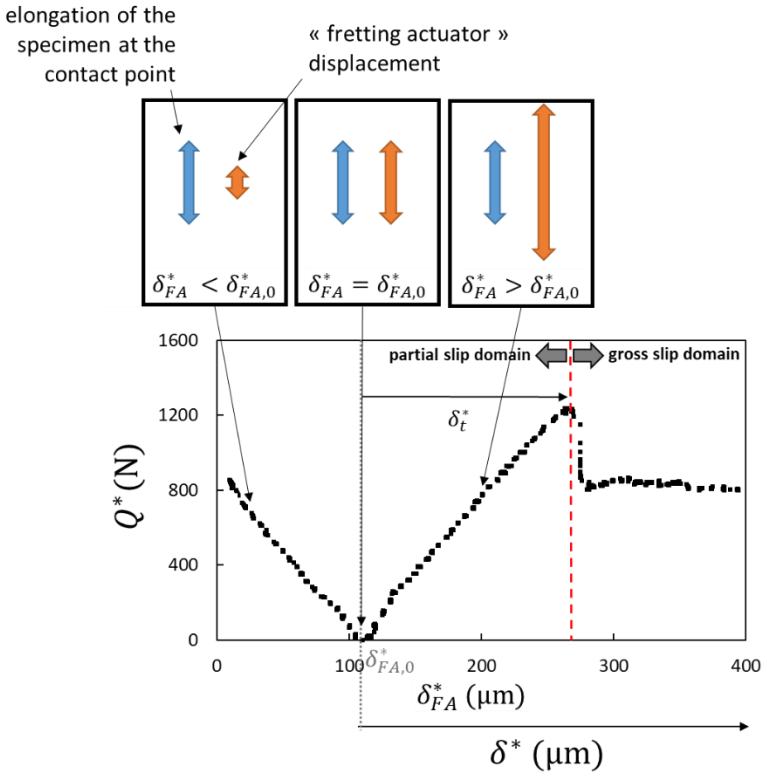

Figure 3 : illustrated variable displacement test on bright wires with fatigue load. P = 1400 N, σ_m = 320 MPa, σ_a = 160 MPa

Note that the value of $\delta^*_{FA,0}$ depends on the imposed fatigue stress amplitude. Note also that $\delta^*_{FA,0}$ is null when the fatigue stress amplitude is null. In the following, we simply use the term "displacement amplitude" for δ^*. This value is very useful for the presentation of results, as it discriminates well the loads in both the partial slip and gross slip domains. An explanation of the phenomenons of partial slip and gross slip can be found in [6, 7]. Note that the displacement amplitude scale is rig dependant, as it depends largely on the stiffness of the setup. To compare these results with the tests in the litterature, one must use rig independent variables, such as the tangential force amplitude Q^* (which discriminates the fretting loads only in the partial slip domain), or the sliding amplitude δ^*_s (which discriminates the fretting loads only in the gross slip domain). The sliding amplitude is estimated with the following equation:

$$\delta_s^* = \delta^* - \delta_t^* \cdot \frac{\mu_{GS}}{\mu_t} \qquad (5)$$

where δ^*_t is the displacement amplitude at the partial slip/gross slip transition, μ_{GS} is the friction coefficient in gross slip, and μ_t is the friction coefficient at the partial slip/gross slip transition.

Several series of tests were performed. The normal force was fixed at P = 1400 N and the mean fatigue stress at σ_m = 320 MPa. For an axial tension on the wire rope corresponding to 20% of its minimal rupture tension (which is a conservative assumption of what can be expected in service),

analytical calculations show that the normal forces vary between 100 N in the outer layer to 10 000 N in the inner layer. We chose the normal force in an intermediate layer, partly as some feedback from the industry points that the wire ruptures are more frequent there. Analytical calculations also show that the mean fatigue stress is about the same for all wires at σ_m = 320 MPa.

All tests were conducted in the $\delta^* \geq 0$ domain. In the first (A) and second (B) series of tests, respectively conducted on bright and coated wires, the amplitude of the fatigue stress is kept constant at σ_a = 160 MPa, and the displacement amplitude δ^* is varied from the partial slip domain to the gross slip domain, covering the whole possible domain of tangential loads in service. The value of the amplitude of the fatigue stress σ_a = 160 MPa was obtained through a numerical simulation of the bending of the wire rope, and corresponds to the maximum value for a wire in an intermediate layer. In the third (C), and fourth (D) series of tests, respectively performed on bright and coated wires, the tangential force amplitude is kept constant under partial slip condition at $Q^* \approx 1000$ N while the amplitude of the fatigue stress σ_a is varied. Most tests on bright wires have already been published in [14], but are reproduced here for comparison with the new tests on coated wires. The load conditions and lifetimes of all tests are compiled in Table 2.

These load conditions were chosen as they are representative of the loadings operating within the inner layers of the steel wire ropes, where wire failures were observed.

Figure 4.a displays the studied contact morphology, and Figure 4.b displays a fretting scar on a coated wire specimen after a fretting fatigue test. A 30° angle between the crossed wires induces an elliptical contact zone inclined of 15° compared to the wires axes, as displayed in Figure 4.a. a_X, a_Y are respectively the semi-major and semi-minor contact ellipse radiuses. If the contact is in partial slip, the contact zone is composed of an inner stick zone and an outer slip zone. c_X, c_Y are respectively the semi-major and semi-minor stick zone radiuses. The contact area is given by:

$$A_W = \pi \cdot a_X \cdot a_Y \qquad (6)$$

Pictures of the fretting scars are taken after each test with an optical digital microscope. The ellipses dimensions are measured on the pictures, and the contact area is calculated using equation (6).

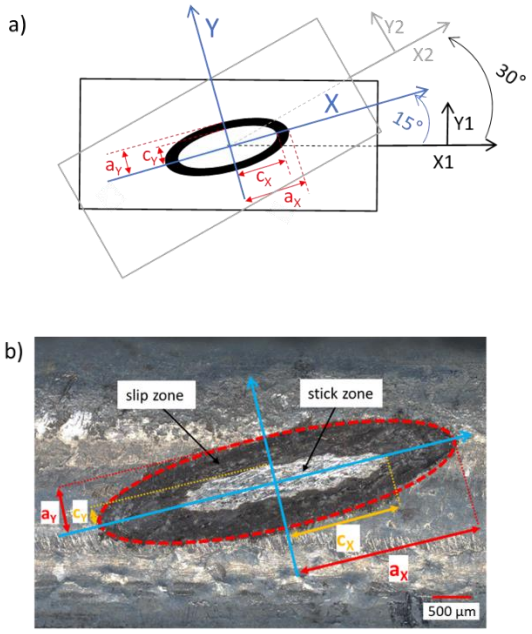

Figure 4 : a) illustration of a fretting scar resulting from the crossed wires contact configuration, b) fretting scar on a coated wire specimen after a partial slip fretting fatigue test

3. Results and discussion

3.1. Influence of fretting and fatigue loads on the fretting fatigue behavior of bright and coated wires

Figure 5 displays the fretting fatigue lifetimes in function of the displacement amplitude for the series with varying fretting load and fixed fatigue load. Several data points are marked ("b" for bright, "c" for coated, with numbers) as they correspond to the tests which will be observed later in the manuscript. Tests were stopped at 10^6 cycles, or at the rupture of the specimen. The observed "U shape" of the lifetime curve is well known (see [10, 12, 23]). Series A has been previously analysed in [14]. For the displacement amplitudes smaller than $\delta^*_{th,b}$ (partial slip condition), the fretting load is too low to induce ruptures. For the displacement amplitudes between $\delta^*_{th,b}$ and δ^*_t (partial slip condition), cracks initiate and propagate until the rupture of the wire. For displacement amplitudes beyond δ^*_t (gross slip condition), wear induces a sharp increase of the contact area, thus a reduction of the contact stresses which reduces the crack initiation risk, promoting longer lifetimes. A similar "U shape" is observed with the Zn coated wires (series B). The displacement amplitude rupture threshold for coated wires $\delta^*_{th,c} \approx 25$ µm is a bit higher than the displacement amplitude rupture threshold for bright wires $\delta^*_{th,b} \approx 20$ µm, but the difference is not very significative. For both bright and Zn coated wires, the minimum fretting fatigue endurance is observed in the partial slip domain just before the gross slip transition, when the tangential force amplitude is maximal and the gross

slip surface wear is not activated. The lifetimes in the partial slip domain between $\delta^*_{th,c}$ and δ^*_t are a bit longer for coated wires, of 100 000 cycles at maximum. In the gross slip domain, lifetime exceeds 10^6 cycles for both bright and Zn coated wires.

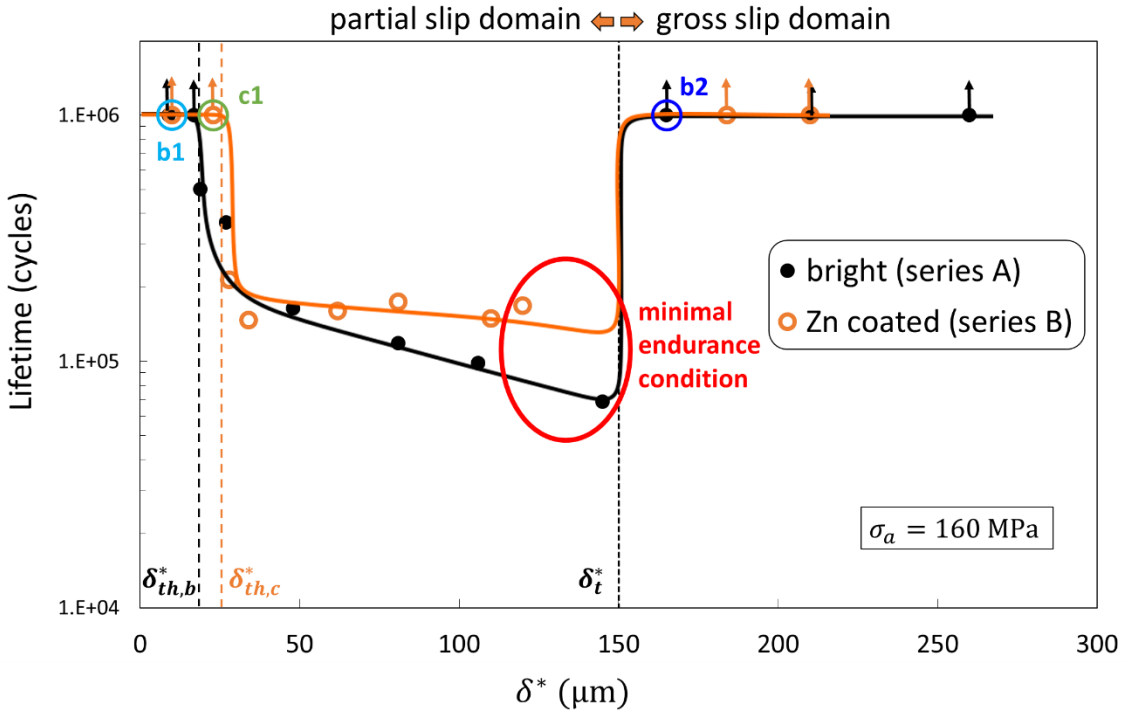

Figure 5 : lifetimes of fretting fatigue tests on bright and zinc coated wires. Fixed fatigue load, varying fretting load. P = 1400 N, σ_m = 320 MPa, σ_a = 160 MPa.

Figure 6 displays chosen fretting loops from fretting fatigue tests on bright and coated wires, with displacement amplitudes across the studied range. Their shapes are typical of contacts in partial slip regime and gross slip regime, as expected. No noticeable difference in the shape of the fretting loops from bright and coated wires is observed. The parallelogram shape of the fretting loops for tests at δ* = 106 µm (Figure 6.b) and δ* = 110 µm (Figure 6.e) is due to the gross slip in the polymer pad / specimen wire contact while the specimen wire / loading wire contact is in partial slip.

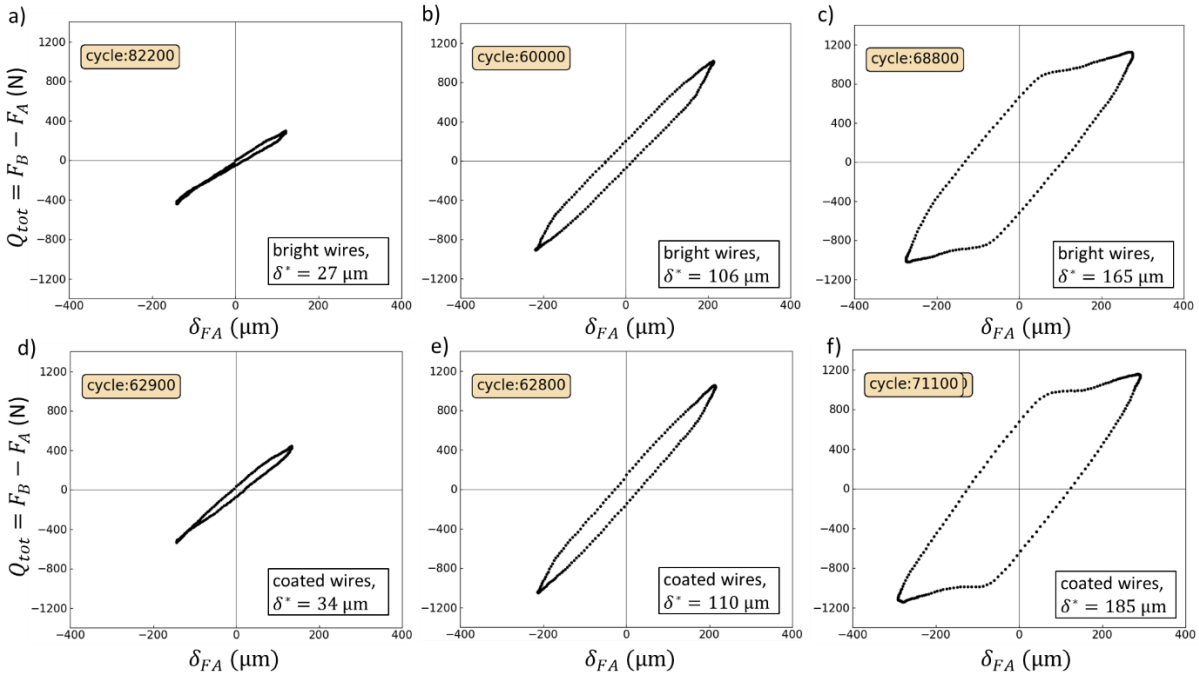

Figure 6: fretting loops for several fretting fatigue tests on bright and coated wires displayed in Figure 5. P = 1400 N, σ_m = 320 MPa, σ_a = 160 MPa.

Figure 7 displays the normalized tangential force amplitudes (averaged over the whole test duration) as a function of the applied displacement amplitude. These are obtained trough a post-processing of the fretting loops. In the partial slip domain, there is an almost linear relationship between the tangential force amplitude and the displacement amplitude. In the gross slip domain, the *Q*/P* ratio is still rising. This increase was previously explained in [14] by a ploughing effect occurring within the fretting scar. The series B curve is approximatively superposed to the series A curve, as the same phenomena are at play. If the setup was infinetly rigid, we should observe a difference in the displacement amplitude for a given tangential force between bright and coated wires, as the zinc coating has a different elastic modulus. But this variation is imperceptible here, as the velocity accomodation is mainly due to the elasticity of the setup (S_0M_0 mode with Daper *et al.* [2] formalism). We note that the expected friction coefficient for zinc to zinc contact is around 0.2, which is significatively lower than the observed friction coefficient of 0.8. This can be explained by a wear of the zinc, so that the contact is actually a steel to steel contact, similar to the contact for bright wires. This hypothesis will be confirmed later.

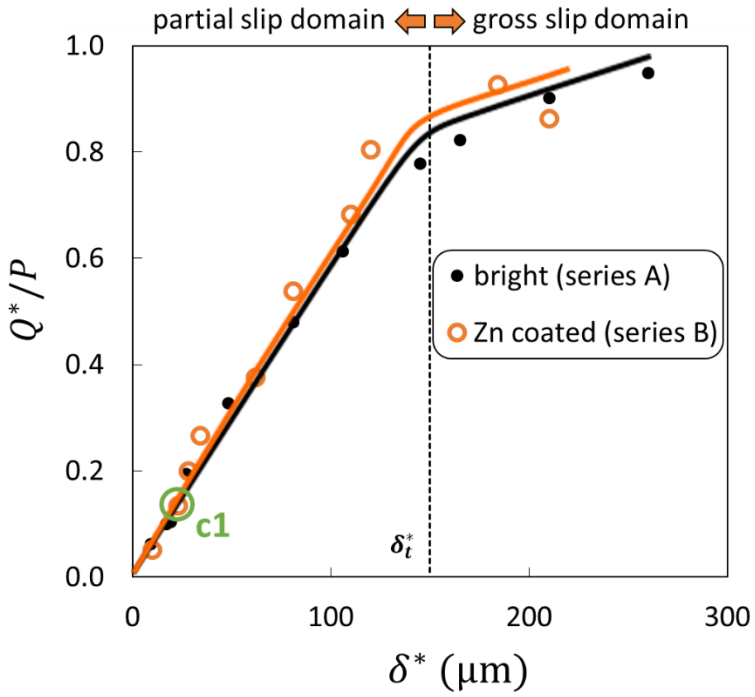

Figure 7 : normalized tangential force amplitudes of fretting fatigue tests on bright and zinc coated wires. Fixed fatigue load, varying fretting load. P = 1400 N, σ_m = 320 MPa, σ_a = 160 MPa

Figure 8 displays the contact areas at the end of the fretting fatigue tests as a function of the applied displacement amplitude. Series A (bright wires) has been analysed in [14]: in the partial slip domain, the final contact area is higher than the contact area calculated with Hertz's theory because of a transient gross slip period during which wear increases the contact area, before stabilizing in partial slip regime. The final contact area increases linearly with increasing *δ**. In the gross slip domain, continuous wear induces an increase of the contact area which follows Archard's law. Series B (coated wires) follows the same tendency, but the final contact areas in partial slip are significatively larger than for bright wires, as observed by Dieng *et al.* [4]. This can be explained by the plastification of the zinc layer, as well as wear of the zinc during the transient gross slip period. This hypothesis will later be confirmed.

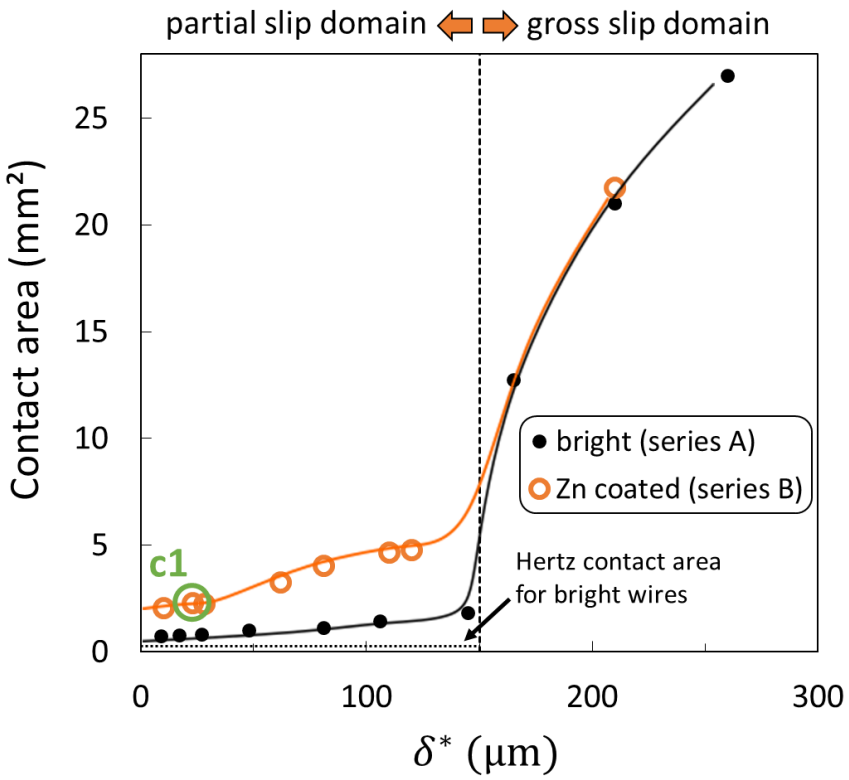

Figure 8 : contact areas at the end of fretting fatigue tests on bright and zinc coated wires. Fixed fatigue load, varying fretting load. P = 1400 N, σ_m = 320 MPa, σ_a = 160 MPa

Figure 9 displays the fretting fatigue lifetimes as a function of the fatigue load amplitude for the series with varying fatigue load and fixed fretting load (P = 1400 N, Q^* ≈ 1000 N). This fretting loading was chosen as the most critical one in Figure 5. The fretting-fatigue limit seem to be close to σ_a = 35 MPa for both bright and coated wires.

Table 2 : load conditions and results for all fretting fatigue tests

Series	bright/coated	P (N)	δ* (μm)	Q^* (N)	slip condition	σ_m (MPa)	σ_a (MPa)	Contact area (mm^2)	lifetime
A	bright	1400	9	88	PS	320	160	0.77	$> 10^6$
A	bright	1400	17	141	PS	320	160	0.77	$> 10^6$
A	bright	1400	19	147	PS	320	160	?	500 000
A	bright	1400	27	273	PS	320	160	0.81	370 000
A	bright	1400	48	460	PS	320	160	1.02	167 000
A	bright	1400	81	673	PS	320	160	1.16	121 000
A	bright	1400	106	860	PS	320	160	1.44	107 000
A, C	bright	1400	145	1090	PS	320	160	1.85	74 000
A	bright	1400	165	1152	GS	320	160	12.76	$>10^6$
A	bright	1400	210	1264	GS	320	160	21.02	$>10^6$
A	bright	1400	260	1330	GS	320	160	27.01	$>10^6$
B	coated	1400	10	73	PS	320	160	2.08	$>10^6$
B	coated	1400	23	190	PS	320	160	2.32	$>10^6$
B	coated	1400	28	281	PS	320	160	2.26	214 000
B	coated	1400	34	374	PS	320	160	?	147 000
B	coated	1400	62	528	PS	320	160	3.28	160 000
B	coated	1400	81	754	PS	320	160	4.04	174 000
B	coated	1400	110	956	PS	320	160	4.69	149 000
B, D	coated	1400	120	1128	PS	320	160	4.81	168 000
B	coated	1400	184	1299	GS	320	160	22.67	$>10^6$
B	coated	1400	210	1208	GS	320	160	21.78	$>10^6$
C	bright	1400		1004	PS	320	100	4.42	223 000
C	bright	1400		953	PS	320	49	3.36	610 000
C	bright	1400		1008	PS	320	36	7.19	1 190 000
C	bright	1400		979	PS	320	35	8.64	3 720 000
D	coated	1400		1043	PS	320	81	4.68	233 000
D	coated	1400		1045	PS	320	54	7.14	575 000

D	coated	1400		986	PS	320	43	7.36	1 170 000
D	coated	1400		1018	PS	320	35	7.48	>3 200 000

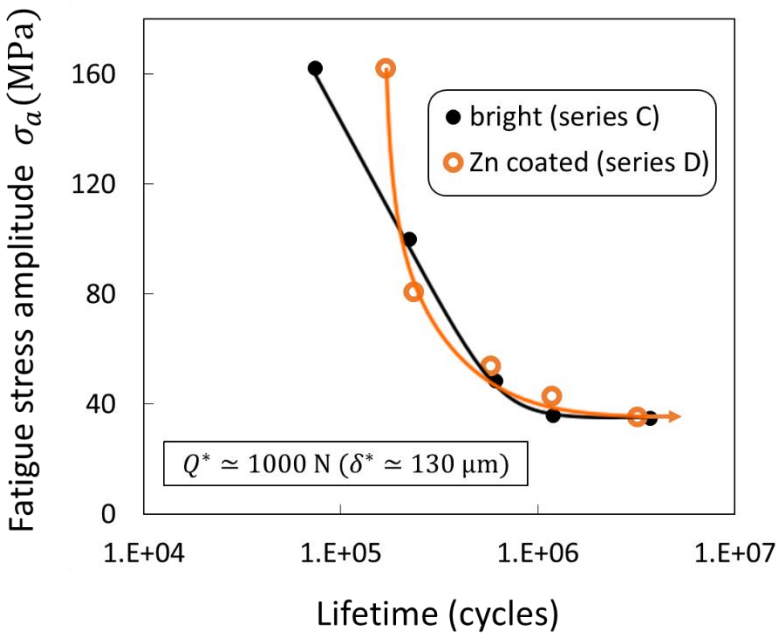

Figure 9 : lifetimes of fretting fatigue tests on bright and zinc coated wires. Fixed fretting load, varying fatigue load. P = 1400 N, σ_m = 320 MPa, Q ≈ 1000 N (δ* ≈ 130 µm)*

Figure 5 and Figure 9 show no significative effect of the zinc layer on the lifetime of the wires. This was expected in the tests of Figure 9, as the variation of lifetime with varying fatigue load is primarily due to the crack propagation kinetics within the wire section, which should be unaffected by a change of composition of the surface of the wires. This was unexpected in Figure 5, as the variation of lifetime with varying fretting load is primarily due to the crack initiation kinetics at the surface of the wires, which should be affected by the zinc layer. Dieng *et al.* [4] do observe a beneficial effect of galvanisation on the fretting fatigue endurance of the wires for the load conditions they studied. They explain this tendency by a larger contact area for coated wires which reduces the contact stresses. In the present investigation, a larger contact area is indeed observed, but it seems to have very little effect on the lifetime. We intend to investigate this surprising result.

3.2. Crack initiation numerical prediction for coated wires.

Using the hybrid numerical model developped for bright wires contact in [14], we calculated the multiaxial fatigue criterion SWT for series B (coated wires). We used the measured contact zone

dimension (Figure 8) and the recorded normal forces and tangential force amplitudes as inputs. The corresponding pressure and shear fields were then analytically calculated. These fields, along with the experimentally imposed fatigue loads, were applied to a FEM model of a wire. This provides the stress field in the wire in function of time, from which the SWT equivalent stress field can be calculated. Finally, the SWT equivalent stress at the critical distance under the hotspot $\sigma_{SWT,ld}$ was extracted. This critical distance was fitted from bright wires tests. Figure 10 displays the experimental lifetimes for tests of series B and the numerically calculated equivalent stress at the critical distance $\sigma_{SWT,ld}$. The equivalent stresses for all tests are inferior to the fatigue limit σ_D, meaning that the model predicts that no crack will ever initiate. The predicted lifetime is thus infinite, which contradicts the experimental data. We conclude that the zinc coating modifies the crack initiation mechanism, so that the model based on bright wires underestimates the risk. A more precise description of the contact interface and the crack initiation mechanism for coated wires is required.

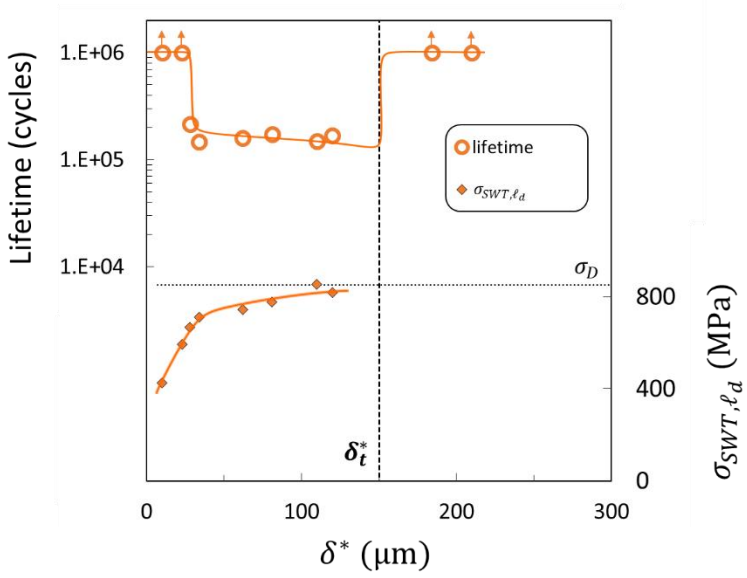

Figure 10 : experimental lifetimes and numerically calculated $\sigma_{SWT,ld}$ for fretting fatigue tests of series B (coated wires)

3.3. Observation of fretting fatigue scars

3.3.1. Bright wires contact

To confirm visually the mechanisms of wear and crack competition, several bright wires specimens were observed.

Figure 11.a displays the fretting scar on the bright wire specimen at the end of fretting fatigue test "b1" (which is indicated in Figure 5). Stick and slip zones are easily visible. Figure 11.b displays a cross section view. A 120 µm crack is observed, initiated in the trailing edge of the fretting scar. The

presence of a crack in a specimen subjected to a fretting load inferior to the rupture/non rupture threshold $\delta^*_{th,b}$ could be explained by one of the following situations :

- This crack is still propagating. Which means that this rupture/non rupture threshold actually is not one, and these tests would end up breaking if continued.
- This crack has stopped propagating. This rupture/non rupture threshold is thus a crack arrest threshold. The maximum crack length attainable with this fretting load is not enough for fatigue to induce propagation until rupture.

It is experimentally difficult to impose lower fretting loads for this set of fatigue loads and normal force and we were not able to determine the crack initiation threshold. It would be interesting to study the crack propagation at these loads to confirm that the crack has indeed stopped propagating. This analysis was unfortunately not possible within the framework of this study. However, the brutal change in lifetimes at the threshold $\delta^*_{th,b}$ seem to indicate a qualitative change in the crack initiation and propagation phenomenon, so that it makes sense to define this value.

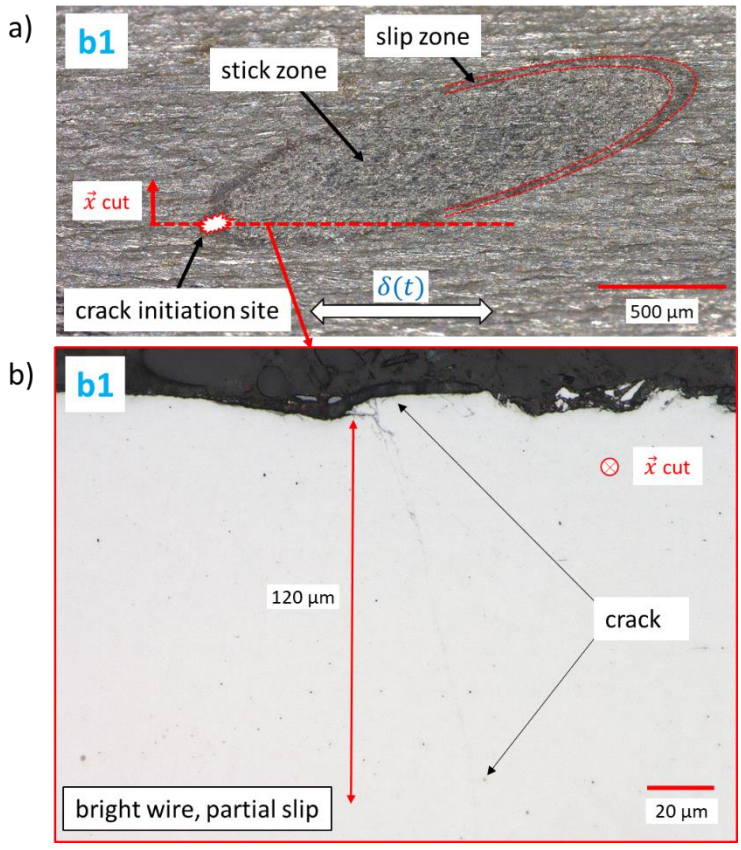

Figure 11 : partial slip fretting fatigue test on bright wires "b1" (indicated in Figure 5) P = 1400 N, σ_m = 320 MPa, σ_a = 160 MPa, δ^* = 10 µm. a) fretting scar at the end of the test, b) longitudinal cross section of the wire.

For the tests in the partial slip domain above $\delta^*_{th,b}$, the failure of the wire complicates the observation of the fretting scar. In order to observe the fretting scar at such fretting loads, and locate the crack initiation site, we interrupted a test after 70 000 cycles, immerged the specimen in liquid nitrogen and broke it (with a Charpy testing machine). Figure 12.a displays the fretting scar of this test. The reddish aspect of the slip zone is characteristic of oxydised iron. This is confirmed in Figure 12.b, which displays an EDX view for oxygen element of this fretting scar. Figure 12.c displays the fractured surface of the corresponding specimen. The semi-circular shape of the crack is visible in Figure 12.c. The observation of the crack confirms that the brittle fracture indeed occured at the crack initiation site. Figure 12.a shows that the crack initiation is located at the trailing edge, which is coherent with the stress field analysis [14].

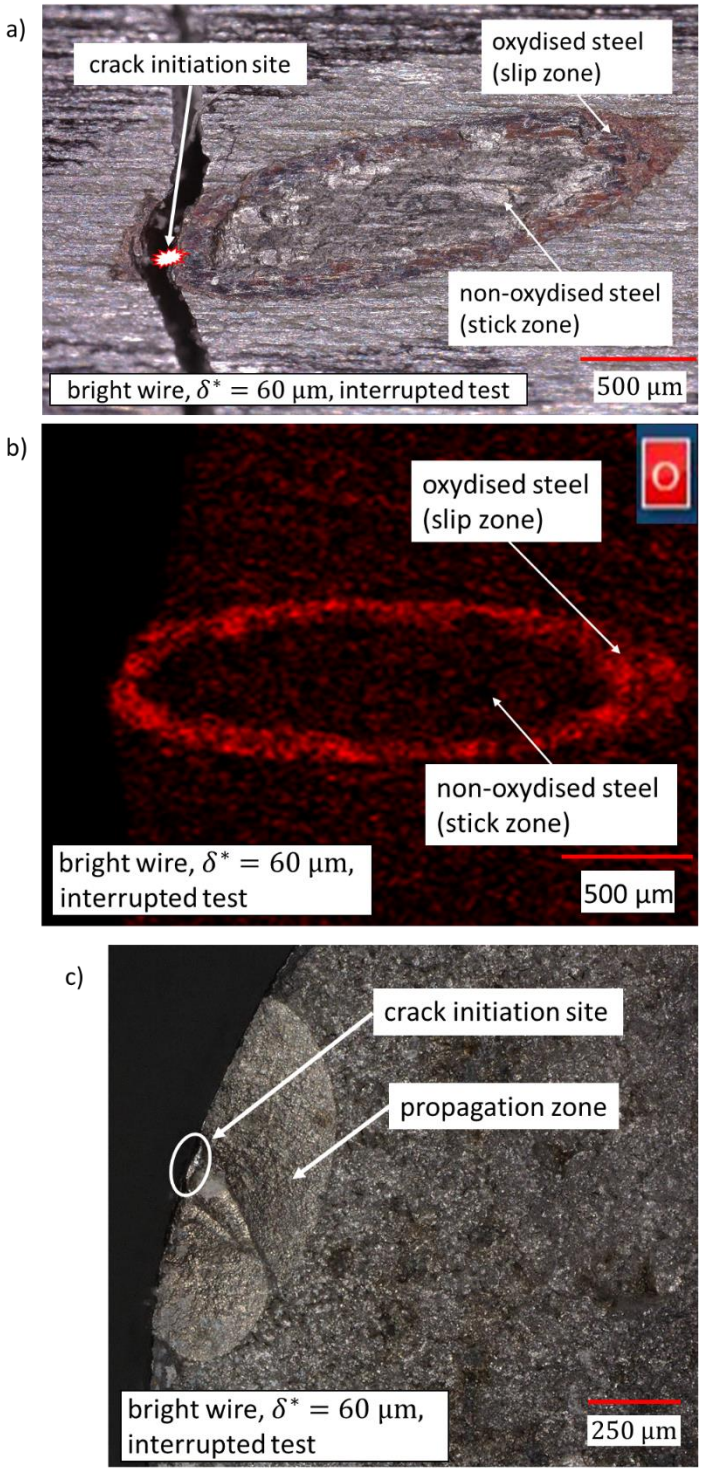

Figure 12 : interrupted partial slip fretting fatigue test on bright wires, later broken with liquid nitrogen. P = 1400 N, σ_m = 320 MPa, σ_a = 160 MPa, δ = 60 µm, 70 000 cycles. a) optical view of the fretting scar at the end of the test, b) EDX view of the fretting scar at the end of the test for oxygen element, c) longitudinal view*

Figure 13.a displays the fretting scar on the bright wire specimen at the end of fretting fatigue test "b2" (Figure 5). Figure 13.b displays a cross section view. In the gross slip domain, wear has two

effects: “rub out” the cracks before they can propagate; and extend the contact area, thus reducing the crack initiation risk. No crack is observed.

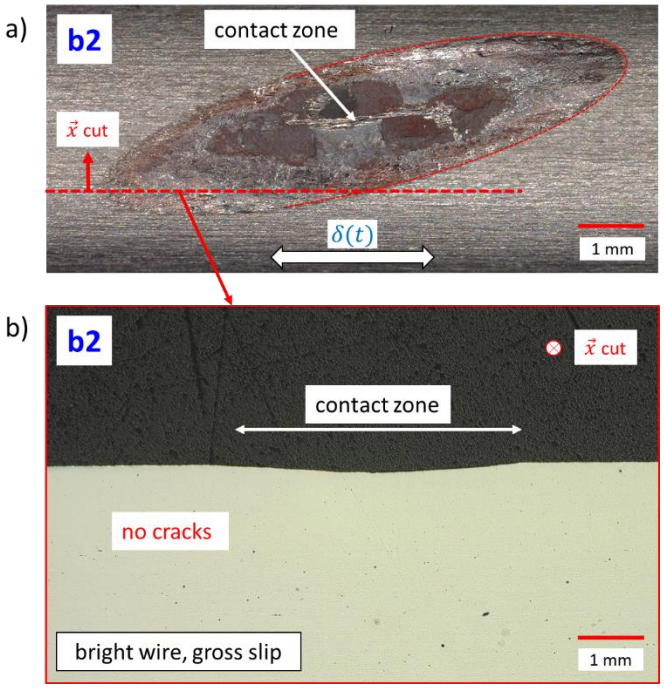

Figure 13 : gross slip fretting fatigue test on bright wires “b2” (indicated in Figure 5). P = 1400 N, σ_m = 320 MPa, σ_a = 160 MPa, δ = 210 µm. a) fretting scar at the end of the test, b) longitudinal cross section of the wire.*

3.3.2. Zn coated wires contact

Figure 14.a displays displays the fretting scar on the coated wire specimen at the end of fretting fatigue test “c1” (Figure 5). Figure 14.b displays a longitudinal cut of this wire. The slip zone is mixed up with a zinc plastic deformation bulge. There seem to be a few cracks in the coating, but they could also be caused by the plastic flow of the zinc being pushed out of the contact, so perhaps they are not “fretting fatigue cracks”. There is no cracks in the steel. It seems that the softer zinc coating, reunites the crack initiation threshold with the non rupture / rupture threshold. Regalla *et al.* [22] explain that soft coating can undergo shear deformation (*i.e.* velocity accomodation), which decreases the shear stress in the substrate (here, the steel) for a given imposed global displacement. This could also be due to the increase in contact area, as hypothesized by Dieng *et al.* [4]. In the stick zone, the coating is deformed but looks smooth, not worn out. The tests conducted by Ramalho *et al.* [18], which show smooth contact surfaces, are probably in this regime. The improved fracture life they observed for coated specimens is qualitatively coherent with the absence of cracks we observe in this coated wire, as well as the small shift in the non rupture / rupture threshold.

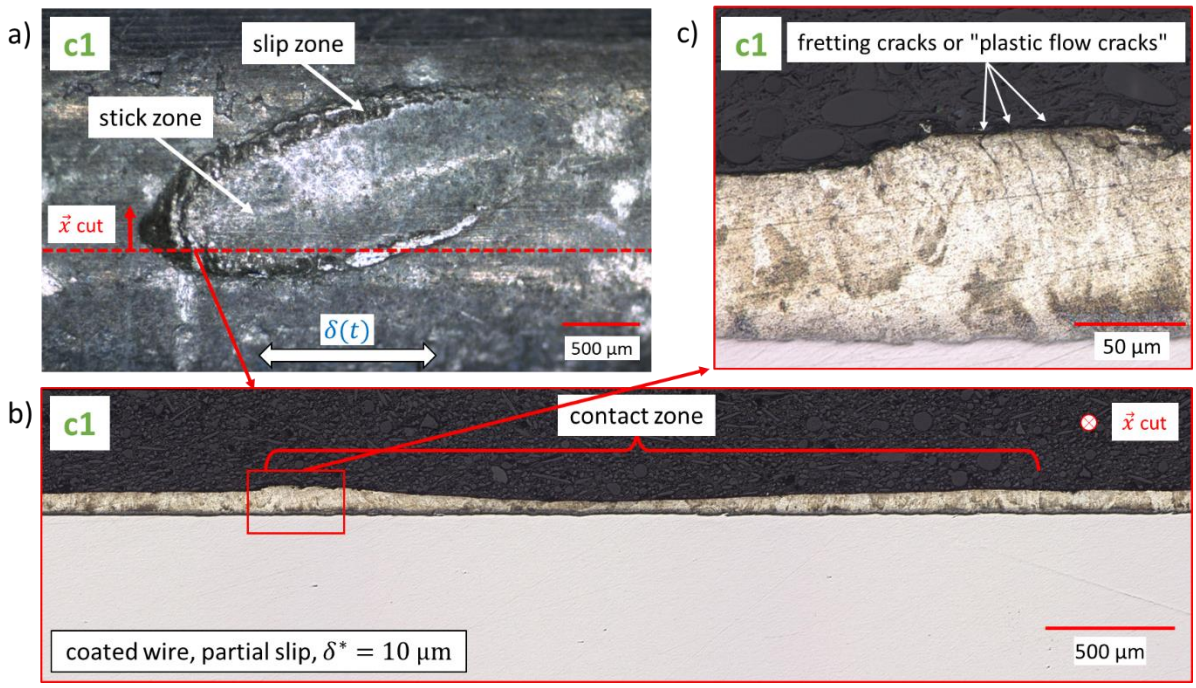

Figure 14 : partial slip fretting fatigue test on coated wires "c1" (indicated in Figure 5) P = 1400 N, σ_m = 320 MPa, σ_a = 160 MPa, δ^* = 10 µm. a) fretting scar at the end of the test, b,c) views of a longitudinal cut of the wire

In the partial slip domain above $\delta^*_{th,c}$, the rupture damages significatively the fretting scar. So, like for tests with bright wires, we interrupted a test after 70 000 cycles and broke it using liquid nitrogen. Figure 15.a displays the fretting scar of this test. The black aspect of the slip zone is due to the oxidised zinc. The asymetry of the slip zone is due to the fatigue stress offset effect explained by Nowell et Hills [16]. We suppose that this asymetry is more visible on coated wires than on bright wires because of the larger contact zone size. The crack initiation is located at the trailing edge, in the center of the slip zone. Some underlying steel is visible in the middle of the stick zone. Figure 15.b displays the fractured surface of the corresponding specimen. The semi-circular propagation zone of the crack is easily visible, as well as the zinc coating layer.

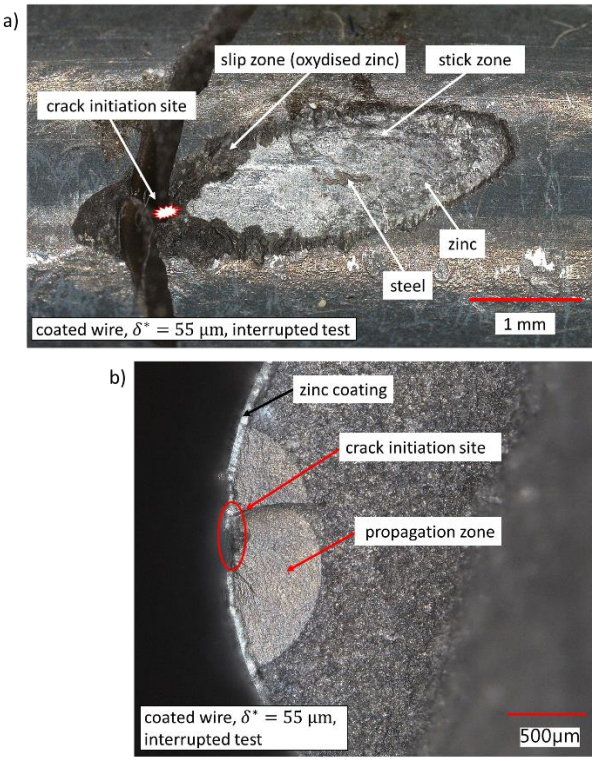

Figure 15 : interrupted partial slip fretting fatigue test on coated wires, later broken with liquid nitrogen. P = 1400 N, σ_m = 320 MPa, σ_a = 160 MPa, δ = 55 µm, 70 000 cycles. a) fretting scar at the end of the test, b) longitudinal view*

3.4. Plain fretting tests for characterization of the fretting scars damages

In order to better understand the absence of effect of the zinc layer on the fretting fatigue endurance, we studied in more detail the wear mechanisms of bright and coated wires, especially in the partial slip domain. Indeed, the fretting fatigue failures damages the fretting scars, making it very difficult to have a precise surface wear assessment of tests from series A, B. Two series of plain fretting tests were conducted, with the same fretting loads as the fretting fatigue tests of Figure 5. These plain fretting series were conducted on the test rig described in paragraph 2.2 with the same protocol, with the exceptions that no fatigue amplitude was applied and that all tests were stopped after 10 000 cycles.

Figure 16.a shows the normalized tangential force amplitude in function of the displacement amplitude for plain fretting tests with bright and coated wires. The partial slip/gross slip transition friction coefficients for bright and coated wires are equal, at $\mu_{t,b} \approx \mu_{t,c} \approx 0.9$, which corresponds to the tribological response derived from the fretting fatigue experiments (Figure 7). The transition friction coefficients observed in the fretting fatigue tests were however a bit lower, at 0.8. In the gross slip domain, the *Q*/P* ratio is at a plateau value around 0.7. The difference with the *Q*/P* ratios observed

in the fretting fatigue tests is due to the short duration of the plain fretting tests (10^4 cycles), as the ploughing effect is much smaller than for the longer fretting fatigue tests(10^6 cycles). The *Q*/P* ratios observed for these short tests correspond to the true gross slip friction coefficients, so that $\mu_{GS,b} \approx \mu_{GS,c} \approx 0.7$. The equalities between these friction coefficients could be due to the complete removal of the zinc layer, so that the contact is actually between steel surfaces in both conditions. Dieng *et al.* [4] do indeed report the wear of the zinc layer prior to the rupture. This will be analysed in the observations of tests A,B,C,D.

Figure 16.b shows the contact areas at the end of the tests. The contact areas in the partial slip domain are coherent with the contact areas observed for the fretting fatigue tests (Figure 8). We showed in [14] that for bright wires, during a transient gross slip period, the contact area increases due to wear. Once the contact has stabilized in partial slip regime, the contact area size is fixed. The same phenomenon is taking place for the coated wires. A sudden increase in contact area evolution as a function of the displacement amplitude is observed around $\delta^* = 60$ µm. This increase is actually also visible in Figure 8. We make the hypothesis that the zinc layer is completely removed for tests with displacement amplitudes above this value.

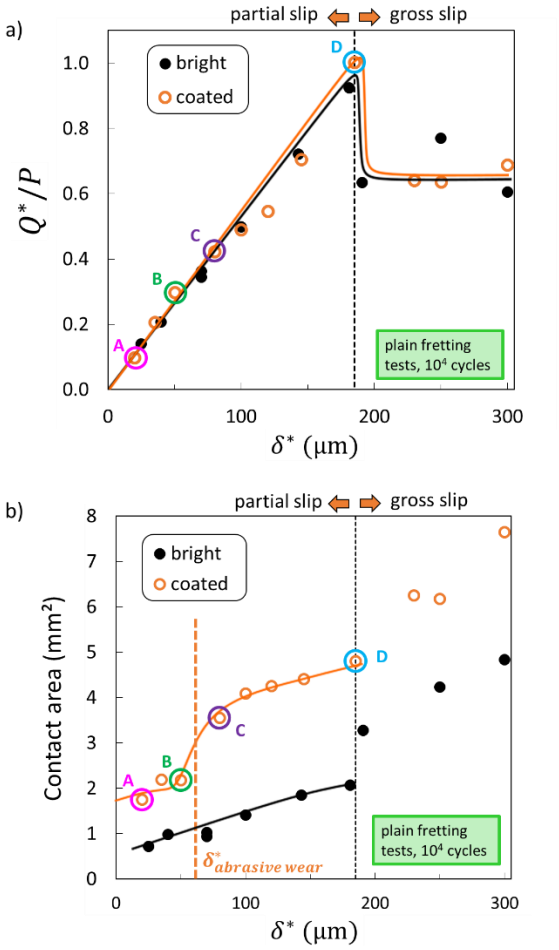

Figure 16 : plain fretting tests on bright wires and coated wires. P = 1400 N, 10 000 cycles. a) normalized tangential force amplitude means, b) contact areas at the end of the tests, in function of effective displacement amplitudes

3.5. Observations of coated wires after plain fretting tests

Figure 17.a displays the fretting scar on the wire at the end of plain fretting test “A”. Figure 17.b displays a view of the corresponding cross section. Like in fretting fatigue test c1, the zinc layer is deformed but not worn out. In the stick zone, the zinc does not look worn out. On the edges of the contact area, a zinc bead is visible. We make the hypothesis that for low displacement amplitudes, the contact area extension is due to the plastic deformation of the zinc. Figure 17.c illustrates the mechanism of the contact area extension for low displacement amplitudes ($\delta^* < \delta^*_{\text{abrasive wear}}$).

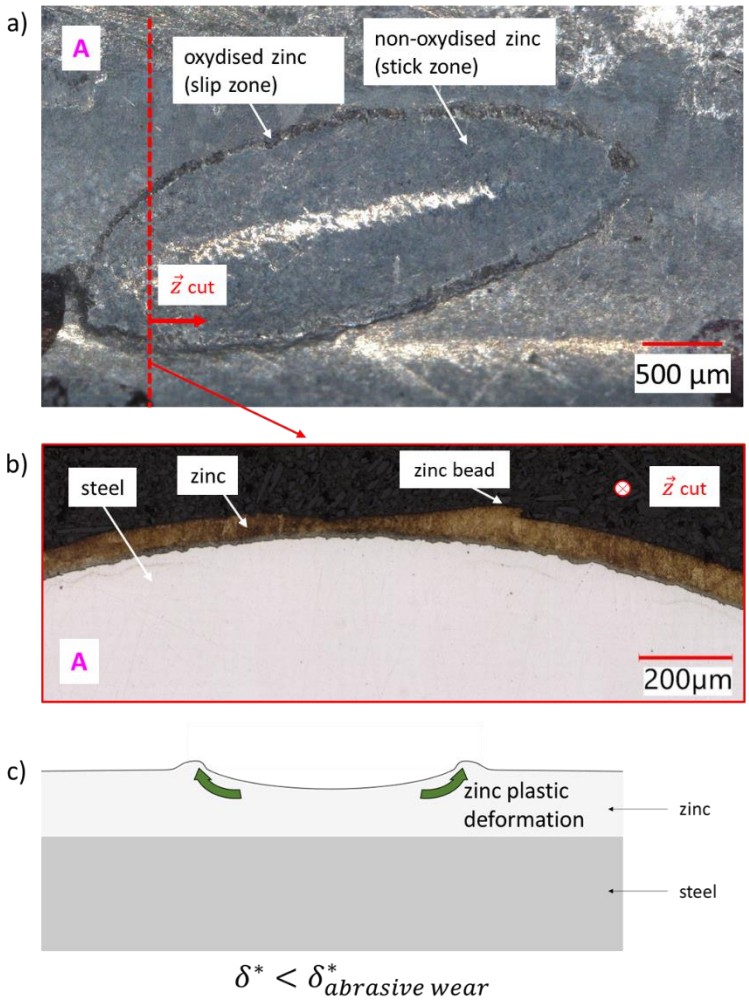

Figure 17 : partial slip plain fretting test on coated wires "A" (Figure 16). P = 1400 N, δ = 20 µm, Q* = 130 N, 10 000 cycles. a) fretting scar at the end of the test, b) view of a transverse cross section of the wire. c) Illustration of the contact area extension mechanism for low displacement amplitudes*

Figure 18 displays an optical view of the surface (a) and cross section (b) of the wire at the end of plain fretting test "B". Figure 18.c displays an EDX view of the iron, zinc and oxygen elements surface distribution. In the stick zone, the zinc is not oxydised, as revealed by its grey color in Figure 18.a and through the EDX view in Figure 18.c. But contrary to test A, zinc has a worn out aspect. Figure 18.b shows that the width of the zinc layer is reduced, but that it is not completely worn out. On the edges of the contact area, a zinc bead probaly due to plastic deformation is visible. We can therefore assume that for intermediate partial slip displacement amplitudes, the contact area extension is due to both plastic deformation of the zinc and abrasive wear during the initial transient gross slip period (Figure 18.d).

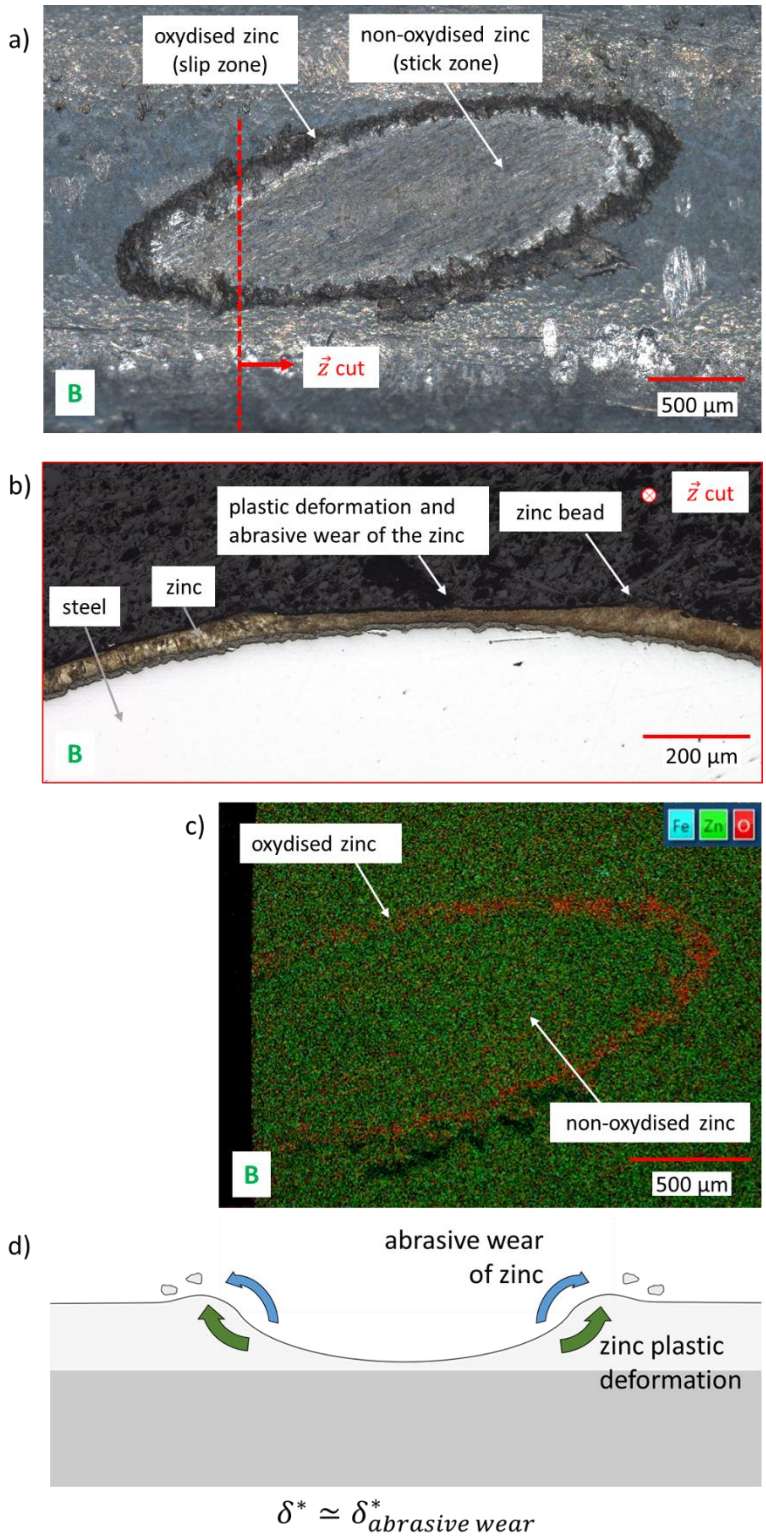

Figure 18 : partial slip plain fretting test on coated wires "B" (indicated in Figure 16). P = 1400 N, δ = 50 µm, Q* = 400 N, 10 000 cycles. a) optical view of the fretting scar at the end of the test, b) view of a transverse cut of the wire, c) EDX view of the fretting scar for iron, zinc and oxygen elements. d) illustration of the contact area extension mechanism for intermediate displacement amplitudes*

Figure 19 displays an optical view of the surface (a) and cross section (b) of the wire at the end of plain fretting test "C". Figure 19.c displays an EDX view of the iron, zinc and oxygen elements

corresponding surface distribution. The stick zone visible in Figure 19.a has a shiny grey aspect typical of zinc, while at first glance to Figure 19.b, the zinc layer seem to have been worn out. But the Zn-Fe compound layer is actually still present over most of the surface, which is visible in the zoomed view in Figure 19.b. The EDX view confirms the presence of zinc over most of the surface, with some iron emerging at the outer edge of the stick zone. We make the hypothesis that the Zn-Fe compound layer has a better resistance to wear than the pure zinc layer, while still containing mostly zinc so that its iron component is not clearly visible with EDX. It seems that for $\delta^* > \delta^*_{\text{abrasive wear}}$, the displacement amplitude is large enough to wear out the pure zinc layer during the initial transient gross slip period. In the rotating tests (thus in gross slip regime) done by Regalla *et al.* [22], the zinc coating was quickly worn out, so that this was to be expected. This qualitative change in the wear mechanism can explain the discontinuity in the evolution of the contact area for $\delta^* = \delta^*_{\text{abrasive wear}}$.

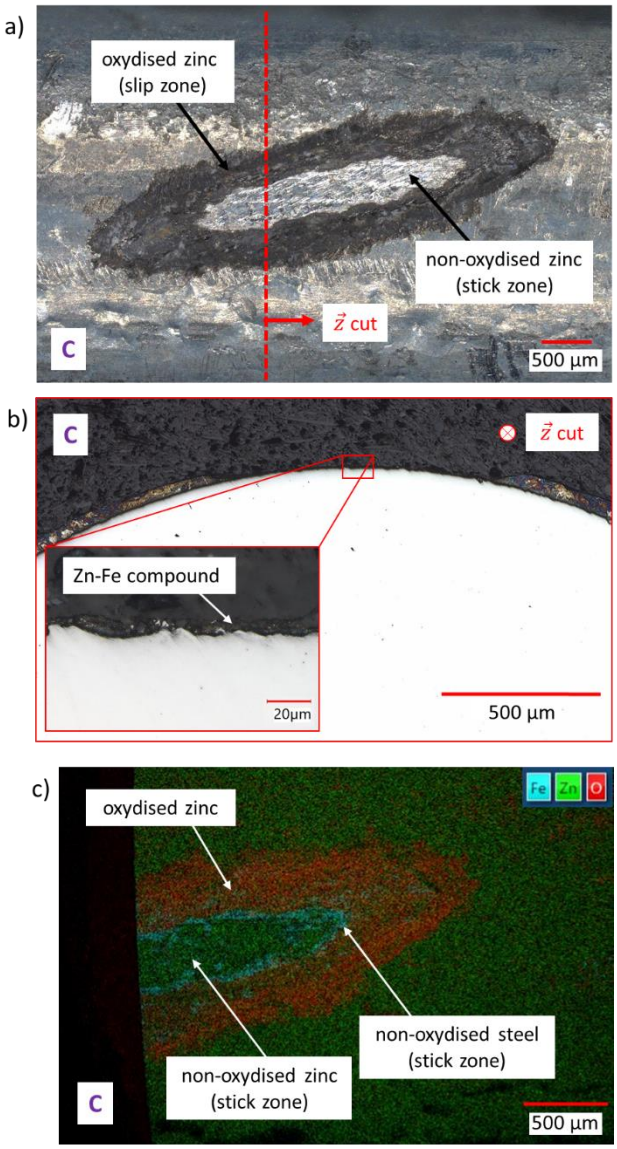

Figure 19 : partial slip plain fretting test on coated wires "C" (indicated in Figure 16). P = 1400 N, δ = 80 µm, Q* = 550 N, 10 000 cycles. a) optical view of the fretting scar at the end of the test, b) view of a transverse cross section of the wire, c) EDX view of the fretting scar for iron, zinc and oxygen elements*

Figure 20 displays an optical view of the surface (a) and cross section (b) of the wire at the end of plain fretting test "D". Figure 20.c displays an EDX view of the iron, zinc and oxygen elements corresponding surface distribution. Figure 20.a and Figure 20.c show that the slip zone is separated into an outer annulus of oxydised zinc and an inner annulus of oxydised steel. The stick zone is composed of non-oxydised steel. Figure 20.b shows a wear of the steel which is differenciated from the wear of the zinc. Figure 20.d illustrates the mechanism of the contact area extension for large displacement amplitudes ($\delta^* > \delta^*_{\text{abrasive wear}}$).

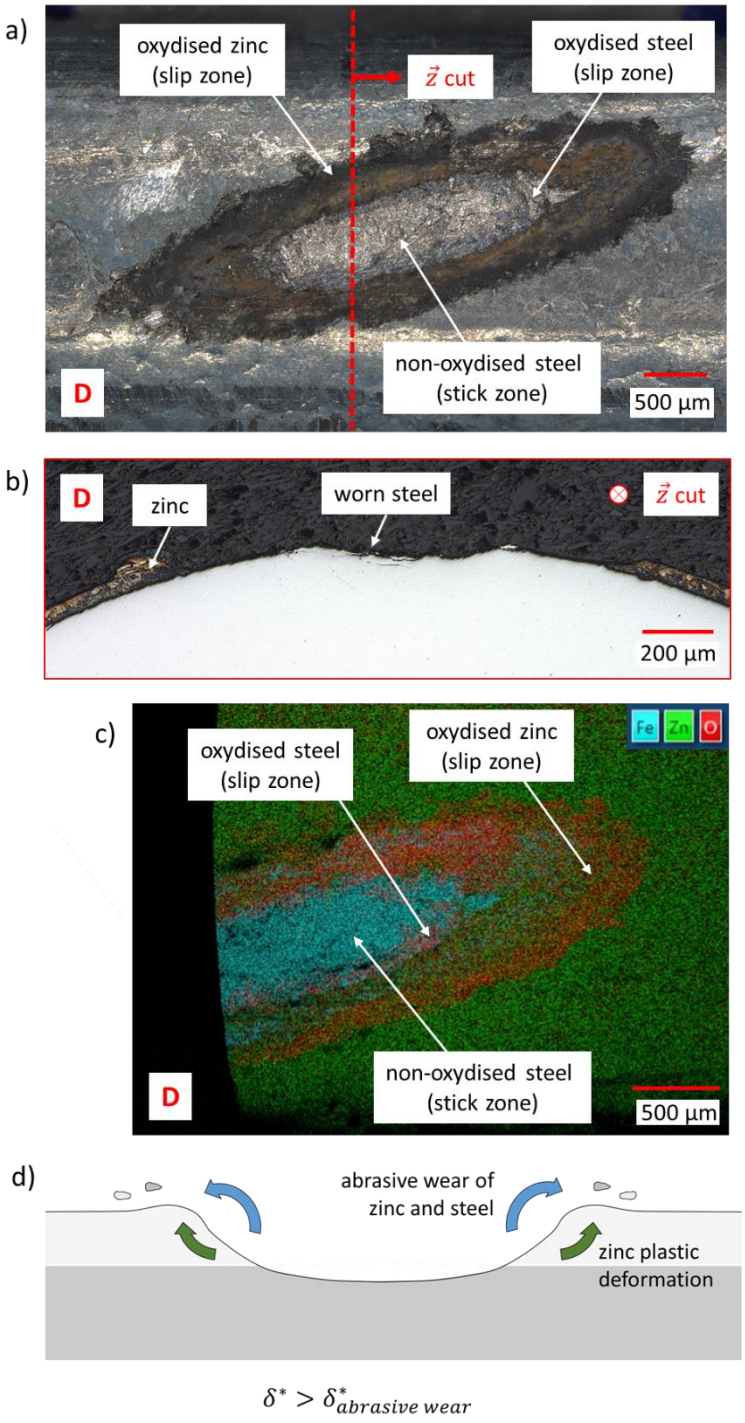

Figure 20 : partial slip plain fretting test on coated wires "D" (indicated in Figure 16). P = 1400 N, δ = 185 µm, Q* = 1350 N, 10 000 cycles. a) optical view of the fretting scar at the end of the test, b) view of a transverse cross section of the wire, c) EDX view of the fretting scar for iron, zinc and oxygen elements. d) illustration of the contact area extension mechanism for large displacement amplitudes*

These observations show that for $\delta^* < \delta^*_{\text{abrasive wear}}$, the zinc deforms plastically essentially because of the normal force. The zinc layer accomodates the tangential displacement and prevents any abrasive wear. For δ^* close to $\delta^*_{\text{abrasive wear}}$, the zinc cannot accommodate anymore and the contact undergoes an initial transient gross slip period, like for bright wires contact. This induces a slight abrasive wear in the zinc layer. For $\delta^* > \delta^*_{\text{abrasive wear}}$, the abrasive wear during this transient gross slip period is enough to expose the Zn-Fe compound layer, and then the steel underneath. Figure 16.b shows that for $\delta^* > \delta^*_{\text{abrasive wear}}$, the increase of contact area as a function of the displacement amplitude for coated wires is similar to the one for bright wires: it's the steel/steel contact that pilots the wear kinetics.

3.6. Discussion

The present investigation focuses on the effect of a zinc coating on steel wires fretting fatigue endurance. For the tests with varying fretting displacement amplitude δ^*, a classical "U shape" endurance curve is observed. Under gross slip conditions, the surface wear reduces the contact stresses and infinite endurance is observed. Under partial slip conditions, limited endurances are observed. Dieng *et al.* [4] have observed a transient initial gross slip period before stabilization of the contact in partial slip, and an increased contact area compared to bright wires contacts, as we did. They also observe a large positive effect of galvanisation on the fretting fatigue limit, which they explain could be due to the observed increase in contact area. Note that Dieng *et al.* tests' were conducted on a single actuator testing machine, so that fatigue and fretting loads are connected. In contrast, in the present work we do not observe a significant effect of the coating on the fretting fatigue limit for tests with fixed fretting loads and varied fretting loads. For tests with fixed fatigue loads and varying fretting loads, we observe only a very small effect of the coating on the rupture/non-rupture threshold compared to the effect observed by Dieng *et al.* According to the numerical model developped with bright wires, the contact areas of galvanised wires should completely prevent crack initiation, which is in contradiction with the observed failures. We try to explain why the model is incorrect, and the difference between Dieng *et al.* results and our experimental results. We propose the following hypothesis, based on our fretting scar observations.

For $\delta^* < \delta^*_{\text{th,c}}$, there is no abrasive wear on zinc coated wires. The soft zinc layer probably accomodates elastically (and perhaps plastically) the relative displacement (S_1M_0 and S_1M_1 modes). For bright wires, non-propagated cracks are observed for these loads. For coated wires, theres are no cracks, as both the increased contact area and the zinc accomodation decrease peak stresses in the steel. For $\delta^* \approx \delta^*_{\text{abrasive wear}}$, the tangential displacement is large enough to induce an initial transient

gross slip period which wears out the zinc layer in the center of the contact zone. The Zn-Fe layer seem to have an higher resistance to wear than pure zinc, but for larger displacement amplitudes the Zn-Fe layer is also worn out. This creates a composite contact configuration, with a steel/steel contact in the center of the contact zone, and a zinc/zinc contact in the outer annulus. Figure 21.a presents an illustration of the pressure and shear profiles used in the numerical model. Those analytically calculated profiles are based on the measured contact zone size, with the underlying hypothesis that the bodies in contact are made of a single material, which is not true here. Figure 21.b presents an illustration of the expected pressure and shear profiles if the lower elastic modulus and lower yield stress of the zinc alloy was considered (composite model). The outer annulus zinc/zinc contact would present lower stresses compared to the inner steel/steel contact. The global normal and tangential force being the same, as well as the contact area, the composite model suggests more localized and thus higher fretting stresses than the classical model. This suggests that merely measuring the contact area is not a good indicator to evaluate the crack initiation risk. The classical model predicts a maximum crack initiation risk at the trailing edge of the contact, while the composite model would predict crack initiations in the contact zone, which is coherent with experimental observations for Zn coated wires (Figure 15). To quantify this hypothesis, it would be necessary to calculate the actual pressure and shear stress profiles, and apply them to a FEM model of a wire which models the mechanical properties of the zinc coating.

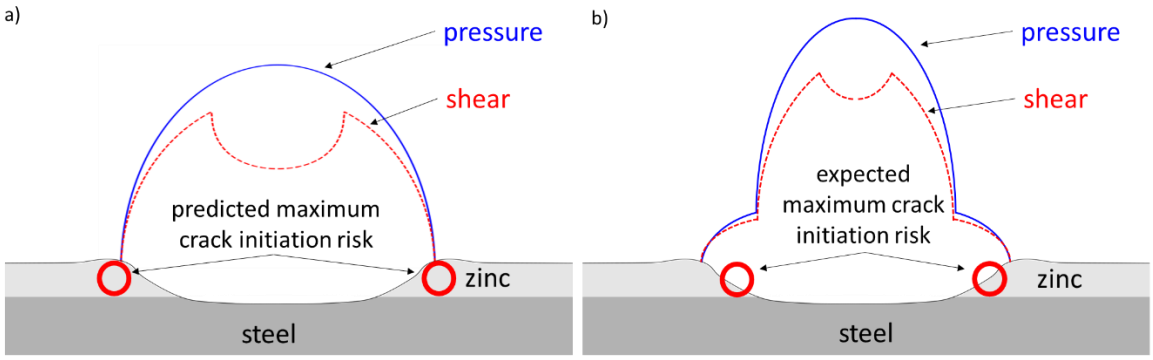

Figure 21 : illustration of a) a classical distribution of pressure and shear profiles, used in the numerical model, and predicted maximum crack initiation risk, b) a composite description of expected pressure and shear considering the higher ductility of the Zn annulus, and expected maximum crack initiation risk

We note that Dieng *et al.* observed an elimination of the zinc layer due to wear prior to any rupture, as well as a remaining Zn-Fe compound layer of 10 µm in one of the tests below the fretting fatigue limit. Given Dieng *et al.*'s results, we could make the hypothesis that the presence of this Zn-Fe compound layer prevents crack initiation. However, in the present results, we observe that crack initiation is prevented only for δ^* inferior to δ^*_{th}, which is significatively smaller than $\delta^*_{abrasive\ wear}$,

which in turn is smaller than the displacement amplitude for which the Zn-Fe layer is completely removed. For example, the interrupted fretting fatigue test of Figure 15 had initiated a crack while the contact zone was mainly composed of zinc. We conclude that there is discrepancy between the results on whether the full zinc layer or only the Zn-Fe layer is required to block crack initiation, but that it could simply be due to the difference in applied loads. Indeed, Dieng *et al.* imposed a normal force of P = 200 N while we imposed a normal force of P = 1400 N. In order to further explore the effect of the Zn-Fe layer on crack initiation prevention, it would be interesting to perform additional interrupted fretting fatigue tests with various normal forces and observe the specimens. In situ observations like X-ray micro-tomography also appear as an interesting alternative to deepen the understanding of such complex fretting fatigue processes [17].

Conclusion

In the present study, we tried to analyse the effects of zinc coating on the lifetime of steel wires under fretting fatigue loads. We largely compared our results to Dieng *et al.* [4] results, as they conducted a similar comparison between bright and coated wires fretting fatigue behavior. The main findings of this work are :

- For very small partial slip fretting displacement amplitudes, the contact area extension of coated wires is induced by plasticity. For displacement amplitudes above a threshold, the contact area extension is monitored by plasticity and abrasive wear of the Zn layer.
- For very small partial slip fretting displacement amplitudes, the zinc coating seem to prevent crack initiations. This may be due to the extended contact area, but also to the accomodation of the shear stresses thanks to the zinc softness.
- The Zn coating leads to a composite contact structure for a large range of displacement amplitudes, with a direct steel/steel interface in the center of the contact surrounded by a Zn/Zn interface annulus.
- Considering that the observed contact area for coated wires influences the contact stresses and crack initiation mechanism in the same way as for bright wires is erroneous, and leads to an underestimation of the risk. This might be due to the softness of the zinc coating, which accomodates shear deformation.
- At least for the tested fretting load (the most critical one), bright and coated wires have the same fretting fatigue limit.

Additional tests would be needed to create an extended fretting fatigue map, but these results show that the expected beneficial effect of the zinc layer can be almost null for certain load conditions. A conservative assumption for rope design would thus be to consider that the zinc is quickly worn out of the contact and has not beneficial effect afterwards.

Acknowledgments

The authors would like to thank the people at the ArcelorMittal factory of Bourg-en-Bresse for providing the wires.

References

[1] R. Chaplin and A. Potts. 1991. *Wire rope offshsore - a critical review of wire rope endurance research affecting offshore applications*. HSE, Offshore Technology Report.

[2] J. Denape, Y. Berthier, and L. Vincent. 2001. Wear Particle Life in a Sliding Contact Under Dry Conditions : Third Body Approach. In *Fundamentals of Tribology and Bridging the Gap Between the Macro- and Micro/Nanoscales*, Bharat Bhushan (ed.). Springer Netherlands, Dordrecht, 393–411. https://doi.org/10.1007/978-94-010-0736-8_28

[3] L. Dieng, V. Périer, L. Gaillet, and C. Tessier. 2009. Mécanismes de dégradation et moyens de protection des câbles du génie civil: Exemple des câbles de haubanage. *Mechanics & Industry* 10, 1 (January 2009), 33–42. https://doi.org/10.1051/meca/2009030

[4] L. Dieng, J.R. Urvoy, D. Siegert, P Brevet, V. Perier, and C. Tessier. 2007. Assessment of lubrication and zinc coating on the high cycle fretting fatigue behaviour of high strength steel wires. In *How to get the most out of your ropes*, September 2007. 85–97.

[5] L. J. Fellows, D. Nowell, and D. A. Hills. 1997. On the initiation of fretting fatigue cracks. *Wear* 205, 1 (April 1997), 120–129. https://doi.org/10.1016/S0043-1648(96)07302-4

[6] S. Fouvry, P. Kapsa, and L. Vincent. 1996. Quantification of fretting damage. *Wear* 200, 1 (December 1996), 186–205. https://doi.org/10.1016/S0043-1648(96)07306-1

[7] S. Fouvry, Ph. Kapsa, and L. Vincent. 1995. Analysis of sliding behaviour for fretting loadings: determination of transition criteria. *Wear* 185, 1 (June 1995), 35–46. https://doi.org/10.1016/0043-1648(94)06582-9

[8] J.P. Gourmelon. 2002. Fatigue of staying cables, Organisation and results of the research programme. International Organisation for the Study of the Endurance of Ropes. *OIPEEC* Bulletin, (2002), 21–39.

[9] R. E. Hobbs and M. Raoof. 1994. Mechanism of fretting fatigue in steel cables. *International Journal of Fatigue* 16, 4 (June 1994), 273–280. https://doi.org/10.1016/0142-1123(94)90341-7

[10] O. Jin and S. Mall. 2004. Effects of slip on fretting behavior: experiments and analyses. *Wear* 256, 7 (April 2004), 671–684. https://doi.org/10.1016/S0043-1648(03)00510-6

[11] L. Lee, S. Descartes, and R. R. Chromik. 2018. Comparison of fretting behaviour of electrodeposited Zn-Ni and Cd coatings. *Tribology International* 120, (April 2018), 535–546. https://doi.org/10.1016/j.triboint.2018.01.021

[12] J. J. Madge, S. B. Leen, I. R. McColl, and P. H. Shipway. 2007. Contact-evolution based prediction of fretting fatigue life: Effect of slip amplitude. *Wear* 262, 9 (April 2007), 1159–1170. https://doi.org/10.1016/j.wear.2006.11.004
[13] J. Meriaux, S. Fouvry, K. J. Kubiak, and S. Deyber. 2010. Characterization of crack nucleation in TA6V under fretting–fatigue loading using the potential drop technique. *International Journal of Fatigue* 32, 10 (October 2010), 1658–1668. https://doi.org/10.1016/j.ijfatigue.2010.03.008
[14] S. Montalvo, S. Fouvry, and M. Martinez. 2023. A hybrid analytical-FEM 3D approach including wear effects to simulate fretting fatigue endurance: Application to steel wires in crossed contact. *Tribology International* 187, (September 2023), 108713. https://doi.org/10.1016/j.triboint.2023.108713
[15] D. Nowell, D. Dini, and D. A. Hills. 2006. Recent developments in the understanding of fretting fatigue. *Engineering Fracture Mechanics* 73, 2 (January 2006), 207–222. https://doi.org/10.1016/j.engfracmech.2005.01.013
[16] D. Nowell and D. A. Hills. 1987. Mechanics of fretting fatigue tests. *International Journal of Mechanical Sciences* 29, 5 (January 1987), 355–365. https://doi.org/10.1016/0020-7403(87)90117-2
[17] H. Proudhon, J-Y. Buffière, and S. Fouvry. 2007. Three-dimensional study of a fretting crack using synchrotron X-ray micro-tomography. *Engineering Fracture Mechanics* 74, 5 (March 2007), 782–793. https://doi.org/10.1016/j.engfracmech.2006.06.019
[18] A. Ramalho, L. M Correia, and J. D Costa. 2000. Fretting fatigue of zinc coated low carbon steel EN H320 M. *Tribology International* 33, 11 (November 2000), 761–768. https://doi.org/10.1016/S0301-679X(00)00119-5
[19] M. Raoof. 1990. Axial Fatigue of Multilayered Strands. *Journal of Engineering Mechanics* 116, 10 (1990). https://doi.org/10.1061/(ASCE)0733-9399(1990)116:10(2083)
[20] M. Raoof. 1990. Free Bending of Spiral Strands. *Journal of Engineering Mechanics* 116, 3 (March 1990). https://doi.org/10.1061/(ASCE)0733-9399(1990)116:3(512)
[21] M. Raoof and R. E. Hobbs. 1988. Analysis of Multilayered Structural Strands. *Journal of Engineering Mechanics* 114, 7 (July 1988). https://doi.org/10.1061/(ASCE)0733-9399(1988)114:7(1166)
[22] S. P. Regalla, V. Krishnan Anirudh, and S. K. R. Narala. 2018. Tribological performance of Zinc soft metal coatings in solid lubrication. *IOP Conf. Ser.: Mater. Sci. Eng.* 346, (April 2018), 012022. https://doi.org/10.1088/1757-899X/346/1/012022
[23] O. Vingsbo and S. Söderberg. 1988. On fretting maps. *Wear* 126, 2 (September 1988), 131–147. https://doi.org/10.1016/0043-1648(88)90134-2
[24] D. Wang, D. Zhang, and S. Ge. 2011. Fretting–fatigue behavior of steel wires in low cycle fatigue. *Materials & Design* 32, 10 (December 2011), 4986–4993. https://doi.org/10.1016/j.matdes.2011.06.037
[25] R. B. Waterhouse, M. Takeuchi, and A. P. van Gool. 1989. The relative effects of hot-dip galvanising and electrodeposited zinc on the fretting-fatigue behaviour of roping steel wires in seawater. *Transactions of the IMF* 67, 1 (1989), 63–66. https://doi.org/10.1080/00202967.1989.11870842
[26] R.B. Waterhouse. 2002. Fretting in steel ropes and cables - A review. *ASTM Special Technical Publication* 1425, (January 2002), 3–14.
[27] ISO 16120-2:2017 Non-alloy steel wire rod for conversion to wire - Part 2: Specific requirements for general purpose wire rod. Retrieved from https://cdn.standards.iteh.ai/samples/63742/6db54b538a384800a30e9d0cc40b43a0/ISO-16120-2-2017.pdf